

This work was written as part of one of the author's official duties as an Employee of the United States Government and is therefore a work of the United States Government. In accordance with 17 U.S.C. 105, no copyright protection is available for such works under U.S. Law.

Public Domain Mark 1.0

<https://creativecommons.org/publicdomain/mark/1.0/>

Access to this work was provided by the University of Maryland, Baltimore County (UMBC) ScholarWorks@UMBC digital repository on the Maryland Shared Open Access (MD-SOAR) platform.

Please provide feedback

Please support the ScholarWorks@UMBC repository by emailing scholarworks-group@umbc.edu and telling us what having access to this work means to you and why it's important to you. Thank you.

Total ozone mapping spectrometer retrievals of noon erythemal-CIE ultraviolet irradiance compared with Brewer ground-based measurements at El Arenosillo (southwestern Spain)

M. Antón,¹ V. E. Cachorro,² J. M. Vilaplana,³ N. A. Krotkov,⁴ A. Serrano,¹ C. Toledano,² B. de la Morena,³ and J. R. Herman⁵

Received 2 March 2006; revised 13 December 2006; accepted 17 January 2007; published 7 June 2007.

[1] During the last decade, methods have been developed for estimating ultraviolet (UV) irradiance reaching the Earth's surface using satellite-measured backscattered UV radiances. The aim of this work is to compare UV products (version 8), noon erythemal Commission Internationale de l'Eclairage (CIE)-UV irradiance (and daily CIE UV doses) from NASA Total Ozone Mapping Spectrometer (TOMS), with ground-based measurements from a well-calibrated Brewer spectrophotometer. This system is installed at the ESAt-“El Arenosillo” (Huelva) station, located in southwest Spain, near the Gulf of Cadiz, an area that is exposed to terrestrial Atlantic-Mediterranean air masses, with a high frequency (about 50%) of cloud-free days. The period analyzed was from 2000 to 2004, separated into two periods, 2000–2002 and 2003–2004, for comparative analysis. The reason for the two periods is the known calibration problem of Earth Probe-TOMS that became more pronounced by the end of 2002. The calibration errors are most important in the reflectivity and Aerosol Index TOMS data. Although the comparison results are slightly better for the first period, we do not observe major discrepancies during the second period; thus both periods were combined for final conclusions. Four different atmospheric conditions are tested in order to analyze the effects of clouds and aerosols on the differences between TOMS and Brewer data: all-sky, cloud-free with any aerosols, as well as with low and high aerosol loads. In general, under all sky conditions, TOMS overestimates the noon CIE irradiance by $7.5 \pm 0.7\%$ (daily CIE doses $8.3 \pm 0.6\%$), but the most relevant is that the bias becomes negative for high values of TOMS reflectivity (thick clouds or high cloud optical depth) with a significant noise increase. Therefore the TOMS bias is higher for cloud-free days, $11.8 \pm 0.2\%$, increasing with the aerosol optical depth, as measured by a colocated Cimel-AERONET Sun photometer. A high correlation between TOMS and Brewer CIE noon irradiances was observed when aerosol-binned data are considered, reaching $R^2 = 0.8$. For low aerosol load [aerosol optical thickness (AOT) < 0.1], the TOMS bias of noon CIE data decreases to $8.2 \pm 0.4\%$ while for high load (AOT > 0.25 and α -Angstrom < 0.8 ; mostly due to desert dust events), the bias increases to $15.1 \pm 0.6\%$. This is due to the fact that absorbing aerosols in the boundary layer are currently not adequately modeled in the operational TOMS UV algorithm. TOMS data can be corrected off-line if the absorption part of the aerosol optical thickness (AAOT) is known at the site. However, currently there are no standard methods of measuring AAOT (or aerosol single-scattering albedo) in the UV wavelengths even from the ground. The new AAOT product from Ozone Monitoring Instrument on board of NASA EOS Aura satellite (launched in July 2004) could be used to reduce the bias along with other improvements. This is currently a subject of ongoing research.

Citation: Antón, M., V. E. Cachorro, J. M. Vilaplana, N. A. Krotkov, A. Serrano, C. Toledano, B. de la Morena, and J. R. Herman (2007), Total ozone mapping spectrometer retrievals of noon erythemal-CIE ultraviolet irradiance compared with Brewer ground-based measurements at El Arenosillo (southwestern Spain), *J. Geophys. Res.*, *112*, D11206, doi:10.1029/2006JD007254.

¹Departamento de Física, Universidad de Extremadura, Badajoz, Spain.

²Grupo de Óptica Atmosférica, Universidad de Valladolid, Valladolid, Spain.

³ESAt “El Arenosillo”, Instituto Nacional de Técnica Aeroespacial, Huelva, Spain.

⁴Goddard Earth Sciences and Technology Center, University of Maryland, Baltimore, Maryland, USA.

⁵Laboratory of Atmosphere, NASA/Goddard Space Flight Center, Greenbelt, Maryland, USA.

1. Introduction

[2] The influence of ultraviolet (UV) solar radiation on the biosphere has been broadly studied during the last decades. It is well known that incident UV radiation at Earth's surface has specific effects on terrestrial and aquatic ecosystems [Diffey, 1991]. Moreover, this radiation can cause harmful effects on human health (skin cancer, cataracts, or immunological impacts). Increases in UV-radiation exposure combined with more outdoor activities have favored a fast rise in those negative effects. According to the *American Cancer Society (ACS)* [2004], during the 1970s, the incidence rate of melanoma (the most dangerous type of skin cancer) rose rapidly at about 6% per year in the USA, although the incident rate slowed to a little less than 3% per year after 1981. Therefore there is a great interest in the analysis of UV radiation values and trends at different locations.

[3] Long-term ground-based and satellite UV data sets have been utilized for detecting trends in UV radiation and for establishing its climatology [World Meteorological Organization, (WMO), 2003 and references therein]. Surface UV-monitoring stations are sparsely located, and most of them have been operating for a relatively short time, which is not sufficient for trend analysis (i.e., >10 years). Moreover, the ground-based measurements have been made using a variety of instruments with different calibration procedures [Leszczynski et al., 1998; WMO, 1996]. Satellite data complement ground-based measurements providing global daily maps with uniform spatial coverage using single instrument. Most importantly, long-term satellite climate-quality UV data records exist such as NASA's Total Ozone Mapping Spectrometer (TOMS, <http://toms.gsfc.nasa.gov>), which are based on similar (although not identical) well-calibrated instruments [McPeters et al., 1998; Herman et al., 1999; Krotkov et al., 2002]. The combined TOMS UV data record is based on data from two satellite UV spectrometers: Nimbus-7/TOMS instrument (1978–1993) and Earth Probe (EP) TOMS instrument (1996–2005). Satellite UV estimates are averages over large areas (100–200 km) and represent average atmospheric and terrain conditions over such areas. The ground-based measurements are representative of local conditions and are affected by immediate surroundings (buildings, trees). This can be an advantage or disadvantage, depending on the overall goals of UV measurements.

[4] In any case, ground-based instruments provide a direct measure of the surface UV radiation, limited only by calibration and instrumental stability. Satellite UV spectrometers are typically very stable instruments, but they measure backscattered UV irradiance emerging at the top of the atmosphere and derive atmospheric transmittance from radiative transfer models. The models are constrained by simplified assumptions about the atmospheric state that typically assumes horizontally homogeneous conditions and simplified properties of aerosols and clouds. Thus, ground-based and satellite data are complementary tools for monitoring UV radiation and long-term trend estimation.

[5] In recent years, TOMS estimations of erythral UV irradiance (local noon or daily values) have been compared with ground measurements mostly using Brewer spectrometers and also other instruments in different sites; for example, European locations [McKenzie et al., 2001;

Chubarova et al., 2002; Arola et al., 2005; Meloni et al., 2005; Kazantzidis et al., 2006], northern America locations [Herman et al., 1999; Sabburg et al., 2002; Fioletov et al., 2004], New Zealand [McKenzie et al., 2001], and eight stations in Argentina [Cede et al., 2004]. However, there have been no comparisons between TOMS and Brewer UV data in southwest of Europe, although there was another Brewer-TOMS study at Lampedusa Island in the Mediterranean [Meloni et al., 2005]. In this work, such comparison is presented at El Arenosillo (Spain) with a detailed discussion of the possible causes of the differences related with previous results.

[6] The paper is structured as follows: section 2 discusses the satellite and ground-based data used in this study. Section 3 describes the method of the comparison. In section 4, several atmospheric situations are separately analyzed in order to evaluate the effects of clouds and aerosols on the TOMS UV estimations. Finally, section 5 summarizes our conclusions.

2. Data Used in This Study

2.1. Ground-Based UV Measurements

[7] The Atmospheric Sounding Station “El Arenosillo” (ESAt-El Arenosillo) belongs to the Earth Observation, Remote Sensing and Atmosphere Department, Sciences Division, National Institute of Aerospace Technology (INTA). It is located at CEDEA (El Arenosillo Experimental Centre) in Mazagón, Huelva, Spain (37.1°N, 6.7°W, 20 m a.s.l.). This center is integrated in the Global Ozone Observing System (GO3OS) of the Global Atmosphere Watch (GAW) program of World Meteorological Organization (WMO) with number 213. Data gathering, retrieval, and reporting procedures at these stations are standardized by the WMO quality assurance procedures.

[8] The area has a mean of 156 cloud-free days per year [Toledano, 2005] and a uniform and stable surface albedo, which makes this station highly useful for radiometric observations and satellite validation. In fact, it was chosen by the Spanish “Instituto Nacional de Meteorología” (INM) for its Brewer spectrophotometers national network inter-comparison campaigns. In addition, dusty air masses from Africa reach this station during all seasons, most frequently in summer, carrying enormous amount of desert aerosol particles [Cachorro et al., 2005; Toledano, 2005]. This makes the El Arenosillo site particularly valuable for radiation and satellite-validation studies.

[9] The Brewer MK-III double monochromator spectrophotometer measures spectral global UV irradiance between 290 and 363 nm with a sampling of 1 nm but with a spectral resolution [full width at half maximum (FWHM)] ~ 0.65 to ~ 0.45 nm (decreasing with wavelength) and with a wavelength accuracy of ~ 0.05 nm. A complete wavelength scan takes 4.5 min. The wavelength registration of the instrument in terms of micrometer step is checked daily and adjusted from the internal mercury calibration lamp. In addition, Brewer 150 uses a 20-W tungsten-halogen internal standard lamp for determining its relative spectral irradiance response. Moreover, the spectrophotometer is periodically calibrated by comparison with quartz-halogen National Institute of Standards and Technology (NIST) traceable standard lamp (1000-W DXW type) whose relative accu-

racy is 1.56% at 250 nm and 1.12% at 350 nm. This calibration transfer produces systematic uncertainties of $\pm 5\%$ in the Brewer spectral irradiance measurements [Vilaplana, 2004]. Finally, the Brewer 150 is also calibrated every 2 years against a Brewer travelling standard (Brewer 017) from the International Ozone Services (IOS, Canada), previously calibrated against the triad of Brewer spectrophotometers located at the Meteorological Service of Canada (international world reference of Brewer instruments). All these calibration processes guarantee the quality and accuracy of Brewer measurements used in this work to within the specified $\pm 5\%$ tolerance.

[10] A cosine correction has been applied to the measurements using a technique described by Fioletov *et al.* [2002]. First, direct cosine response measurements were made using the irradiance of a standard 1000-W lamp in the ESA_t laboratory. Next, cosine correction function for global irradiance (direct plus diffuse) was estimated, assuming that the instrument's direct cosine response error is independent of the azimuth angle, and diffuse sky radiation is isotropic. Since the effective cloud/aerosol optical thickness (COT) was not measured at our site, it was estimated from Brewer global irradiance measurements as follows:

[11] (1) The lookup table of the normalized global cloud transmittance (CT^{model}):

$$CT^{\text{model}}(\theta, \tau) = \frac{E(\theta, \tau)}{E(\theta, \tau = 0)}$$

was precalculated for different values of solar zenith angles θ and τ using UVspec model [Mayer and Kylling, 2005] and assuming Rayleigh atmosphere, cloud optical thickness (COT) between 0.0 and 3.0 in steps of 0.25, and solar zenith angles from 0 to 80° with a 1° increment.

[12] (2) The measured CT^{Brewer} for each Brewer measurement was estimated as:

$$CT^{\text{Brewer}}(\theta) = \frac{E^{\text{Brewer}}(\theta)}{E^{\text{Cloudless}}(\theta)}$$

where E^{Brewer} is the UV irradiance measured by the Brewer instrument and $E^{\text{cloudless}}$ is the Brewer UV irradiance estimated for cloud-free sky.

[13] (3) Finally, COT at the time of measurement was interpolated from the look-up table CT^{Model} using CT^{Brewer} and θ values as input. In this method, the direct/global ratio is considered null for the cases with COT values higher than 3. This assumption is acceptable since direct irradiance decreases quickly with COT [Fioletov *et al.*, 2002].

[14] Sensitivity studies have shown that uncertainty in the aerosol model produces a very low error (less than 1%) in the global cosine correction factor, which is much smaller than typical bias between satellite and ground-based (GB) UV data. Erythemal UV irradiance values were calculated from the Brewer spectral UV irradiance (angular response-corrected) weighted with the Commission Internationale de l'Eclairage (CIE) erythemal spectrum [McKinlay and Diffey, 1987] as is explained in the works of Vilaplana [2004] and Vilaplana *et al.* [2006].

[15] For aerosol studies, ESA_t-INTA and University of Valladolid operated an automatic Cimel Sun photometer,

which is part of NASA AERONET network (<http://aeronet.gsfc.nasa.gov>). This instrument measures direct sun and sky radiation at four wavelength channels, 440, 670, 870, and 1020 nm (10 nm FWHM for the visible channels) [Holben *et al.*, 1998] and automatic cloud screening [Smirnov *et al.*, 2000]. Only aerosol optical depth (AOD) and the Ångström coefficient (α) from the AERONET direct Sun data (version 1) were analyzed to characterize the aerosol load and type [Cachorro *et al.*, 2006; Toledano, 2005].

[16] The period of measurements analyzed for this study was from January 2000 to September 2004, sampling a wide representative range of atmospheric conditions. Because of the known problem with TOMS calibration affecting data at the end of 2002 (see <http://toms.gsfc.nasa.gov>), we have carried out a preliminary comparative analysis with two separate periods, 2000–2002 and 2003–2004, and later the analysis was extended to the combined period 2000–2004. Errors in Aerosol Index (AI) after 2002 are minimized, since the AI data are filtered by the TOMS project by rejecting all data with $AI < 1$, which also removes a large portion of the incorrect aerosol data. The reflectivity channel has its largest reflectivity errors in the Southern Hemisphere for latitudes poleward of 20°S and much smaller errors at northern midlatitudes. These errors are important for estimating reflectivity trends but not for estimating cloud transmission [$\sim(1 - R)$] by Herman (private communication, 2006).

[17] The most relevant part of this UV comparative analysis is related to aerosol influence because of the high frequency of occurrence of desert dust outbreaks from Africa over this area of the southwest of Spain. A separate study [Toledano, 2005; Toledano *et al.*, 2006] evaluates an inventory of these dust outbreaks over the same period, giving a total of 75 episodes during 319 days, with a mean frequency per year of 15% (63.8 days).

2.2. Satellite TOMS UV Estimates

[18] The TOMS UV algorithm first estimates a cloud-free and aerosol-free surface irradiance (F_{clear}) at solar zenith angles corresponding to the local noon. Next, F_{clear} is corrected by using TOMS estimated cloud and/or non-absorbing aerosol transmittance factor C_T [Krotkov *et al.*, 2001a, 2002]:

$$F_{\text{cloud}} = F_{\text{clear}} C_T \quad (1)$$

where F_{clear} is calculated with a radiative transfer model [Dave, 1964] using TOMS total ozone (version 8) and 360-nm reflectivity data estimated for the instantaneous field of view (FOV) at the TOMS overpass time (morning with approximately 11:30 am local equator crossing time). The ozone and temperature profiles were taken from TOMS climatology (version 7) and the surface albedo from Nimbus-7/TOMS multiyear minimum reflectivity climatology [Herman and Celarier, 1997]. This method is described in literature [Herman *et al.*, 1999; Krotkov *et al.*, 1998, 2001a, 2001b, 2002]. The cloud/aerosol correction (C_T) is calculated in two ways. Typically, the cloud and nonabsorbing aerosol corrections are determined using TOMS reflectivity at 360 nm (R_{360}). This correction is calculated using a plane-parallel cloud model, in which it is assumed that the homogeneous cloud layer is located

between 700 and 500 hPa [Krotkov *et al.*, 2001a]. Alternatively, aerosol absorption effects are estimated using TOMS AI data as described by Krotkov *et al.* [1998] for cloud-free conditions (TOMS reflectivity less than 15%). Algorithm details, including estimates of the various error sources, are given in on-line Algorithm Theoretical Basis Document (ATBD) for the TOMS successor: Ozone Monitoring Instrument (OMI) currently operating on board NASA EOS Aura spacecraft [Krotkov *et al.*, 2001b].

3. Methodology

[19] In this work, both near-noon CIE irradiance and daily CIE dose data sets were compared. For irradiance comparisons, Brewer near-noon CIE irradiance for each day is obtained as unweighted average of all available Brewer erythral UV irradiance measurements between 11:00 and 13:00 (true solar time). The average solar zenith angle (SZA) of Brewer measurements was used instead of the noon SZA in the modified TOMS UV retrieval algorithm in order to estimate Brewer-equivalent TOMS near-noon UV irradiance. For daily CIE dose comparisons, Brewer daily UV doses were obtained by integrating all Brewer measurements over the entire day. In addition, TOMS daily UV doses were generated by integrating TOMS-predicted CIE irradiances at 1-hour intervals between sunrise and sunset using aerosol amounts, cloud reflectivities, and ozone values measured by TOMS at the overpass time. F_{clear} is calculated using the satellite-measured ozone value, and the C_T correction factor [equation (1)] was calculated using the constant value of the effective cloud/aerosol optical thickness derived from a single measurement of backscattered radiance at the time of the satellite overpass [Krotkov *et al.*, 2002].

[20] To determine cloud-free conditions, we use the TOMS Lambertian effective reflectivity (LER) at 360 nm, R_{360} data: A day is considered without clouds when the R_{360} is less than 10% [Kalliskota *et al.*, 2000]. The percentage of such clear days is about 50% of the total. The high percentage of cloudless days shows the prevalence of clear conditions at ESA, although this approach overestimates the frequency of cloud-free days because of possible afternoon clouds not detected by TOMS (overpass solar time ~11:30 am).

[21] Aerosol events were selected according to the aerosol optical thickness (AOT) at 440 nm, AOT_{440} , and Ångström parameter α measured with Cimel Sun photometer. In order to examine the effects of aerosols on differences between satellite and ground-based near-noon CIE irradiances, AOT_{440} and α were averaged between 11:00 and 13:00 true solar time. To analyze the effects of aerosols on daily CIE doses, the AOT_{440} and α were averaged during the day. Two different aerosol conditions were selected: low aerosol load with $\text{AOT}_{440} < 0.1$ and high aerosol load when AOT_{440} and α values were larger than 0.25 and lower than 0.8, respectively. The later values are considered as high turbidity (most of them due to desert dust outbreaks) given the aerosol climatology established by Toledano [2005].

[22] To investigate the effect of clouds and aerosols on the satellite versus ground-based bias, the following data sets were analyzed:

[23] Data set 1: All sky conditions.

[24] Data set 2: Cloud-free cases ($R_{360} < 10\%$) all aerosol conditions.

[25] Data set 3: Cloud-free cases with low aerosol load ($R_{360} < 10\%$ and $\text{AOT}_{440} < 0.1$).

[26] Data set 4: Cloud-free cases with high aerosol load ($R_{360} < 10\%$ and $\text{AOT}_{440} > 0.25$ and $\alpha < 0.8$).

[27] A regression analysis was performed for each data set. Thus regression coefficients, correlation coefficients of determination (R^2), and the root mean square errors (RMSEs) were evaluated for each data set.

[28] In order to compare data sets, the mean bias error (MBE) between TOMS retrievals and ground-based measurements was calculated for each data set. This parameter is obtained by the following expression:

$$\text{MBE} = \frac{1}{N} \sum_{i=1}^N \text{BE}_i \quad (2)$$

where the BEs are defined by

$$\text{BE} = 100 \times \frac{\text{TOMS} - \text{Brewer}}{\text{TOMS}} \quad (3)$$

The uncertainty of MBE is characterized by the standard error SE (also called RMSE):

$$\text{SE} = \frac{\text{SD}}{\sqrt{N}} \quad (4)$$

where N is the number of data and SD is the standard deviation defined by

$$\text{SD} = \sqrt{\frac{1}{N} \sum_{i=1}^N (\text{BE}_i - \text{MBE})^2} \quad (5)$$

4. Results and Discussion

4.1. Data Set 1: All Sky Conditions

[29] Figure 1 shows the scatterplots between TOMS versus Brewer data for near-noon CIE irradiance for the two separate periods 2000–2002 and 2002–2004 (upper panel) and for the whole period 2000–2004 (lower panel). We analyzed the BE separately during these periods in order to observe an effect of the TOMS calibration problem after the end of year 2002. As can be seen, all scatterplots show positive TOMS CIE bias with very similar regression slopes of 1.11, 1.08, and 1.10 as illustrated in Table 1 (for the two separate periods) and Table 2 (for the combined period; first line) with correlation coefficients of 0.94, 0.91, and 0.93, respectively. The differences appear in the intercept, -0.32 for the first period, 6.26 for the second period, and 1.87 for the whole period, which seems to indicate a slightly better agreement for the first period, 2000–2002. The noise, about 30%, similar to that estimated in other works, is given by the RMSE (residual error of the fit), while the second period shows a slightly lower value of 24.8%. Also, in Tables 1 and 2, we show statistical errors of the slope (SLE) and the intercept (INE).

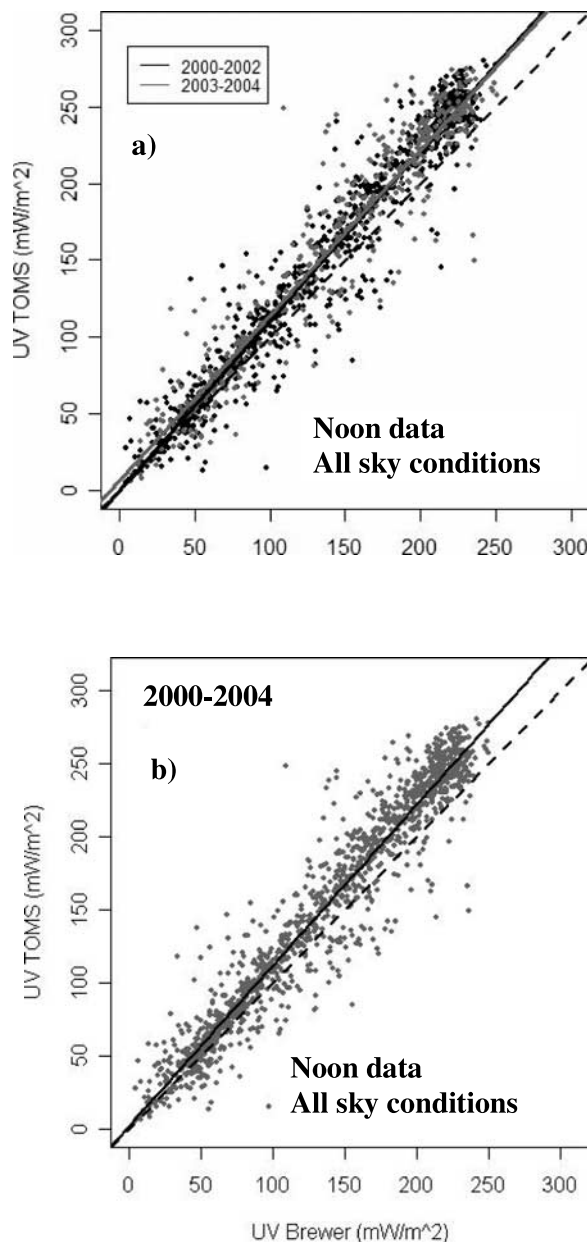


Figure 1. Regression between TOMS and Brewer noon UV irradiance for all sky conditions for the two separate periods, (a) 2000–2002 and 2003–2004 and (b) for the whole period 2000–2004. The solid line is the least square linear regression line, and the dashed line symbolizes the ideal correlation of unit slope.

[30] Since the statistical regression differences are not significant for the two analyzed periods, we have evaluated the temporal evolution of the TOMS bias for the whole period as shown in Figure 2. This figure, which includes all data points and the smoothed moving median, does not show different behavior during the period 2003–2004; therefore in the following sections, the entire period 2000–2004 will be analyzed.

[31] In Table 2, we have also added the results, taking the regression line constrained to pass through the origin and the equivalent results for daily dose (second and fourth lines) in order to compare with previous studies [Kalliskota

Table 1. Results of the Regression Line TOMS Versus Brewer Noon CIE Irradiance for All Sky Conditions for the Two Separate Periods 2000–2002 and 2003–2004

Years	N	Slope	SLE (Slope)	Y Intercept, mW/m ²	INE (Y Intercept), mW/m ²	R ²	RMSE, %
2000–2002	894	1.11	0.01	−0.32	1.10	0.94	32.4
2003–2004	534	1.08	0.01	6.26	0	0.91	24.8

et al., 2000; Chubarova *et al.*, 2002; Cede *et al.*, 2004; Meloni *et al.*, 2005]. Regression parameters for daily dose UV data are very similar to near-noon data, as expected.

[32] The cloud noise in satellite versus ground-based comparisons can be reduced by considering either weekly or monthly mean values [Herman *et al.*, 1999; Kalliskota *et al.*, 2000; Fioletov *et al.*, 2004] or using an ensemble of ground instruments [Williams *et al.*, 2004]. For a single ground instrument, a useful insight can be gained by binning the data with variable cloud conditions according to the TOMS reflectivity (LER) measurements [Krotkov *et al.*, 2001a, 2001b] as shown in Figure 3a for near-noon CIE irradiance. According to Figure 3a, the MBE is ~ 8 –13% for $\text{LER} < 30\%$ but decreases with $\text{LER} > 30\%$ (with increasing variability, note larger error bars given by the $\pm \text{SE}$ of the bin) to about zero for $\text{LER} \sim 35$ –50%. Between $50\% < \text{LER} < 70\%$, biases have positive and negative values, with a strong trend to negative values for $\text{LER} > 70\%$. Figure 3a (bar errors) also shows increased uncertainty when LER increases, in agreement with previous results [i.e., Cede *et al.*, 2004; Kalliskota *et al.*, 2000; Chubarova *et al.*, 2002] and the coefficient of relative variations (CRV), which we explain later.

[33] To gain additional information about TOMS bias, Figure 4 shows similar plots of binned MBE values that are normalized to the Brewer values, although it can be seen that MBE dependence on LER (Figure 4a) becomes less pronounced compared to Figure 3a, especially for high LER cases. This fact is due to TOMS satellite underestimates of the Brewer UV irradiance measurements for high LER values. Thus the MBE values are higher (in absolute value) when the TOMS-Brewer differences are divided by TOMS values than when they are divided by Brewer values.

[34] The TOMS-Brewer differences (BE or MBE), the associated noise (RMSE), and the large error bars calculated from SEs for noon and daily dose data may be in part explained by the different FOV of TOMS and the ground-based site data where the nonhomogeneity and mobility of cloud cover in TOMS-FOV renders an inaccurate match between satellite and ground-based measurements. This

Table 2. Results of the Regression Line TOMS Versus Brewer Noon CIE Irradiance and Daily CIE Dose for All Sky Conditions for the Whole Period 2000–2004^a

	N	Slope	SLE (Slope)	Y Intercept	INE (Y Intercept)	R ²	RMSE, %
Noon	1428	1.10	0.01	1.87 mW/m ²	1.10 mW/m ²	0.93	29.5
		1.11	0.01	0 mW/m ²	0 mW/m ²	0.99	28.9
Dose	1393	1.12	0.01	0.04 kJ/m ²	0.02 kJ/m ²	0.94	27.3
		1.13	0.01	0 mW/m ²	0 mW/m ²	0.98	25.9

^aSecond and fourth lines give the regression line constrained to pass through the origin.

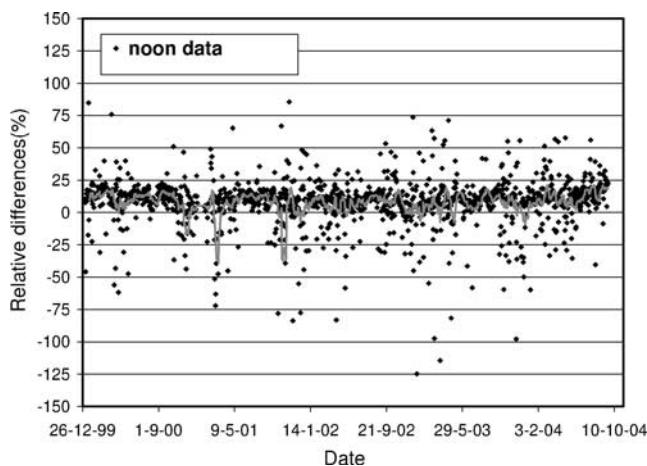


Figure 2. Temporal evolution of the relative differences between TOMS and Brewer (bias TOMS) during the period 2000–2004.

problem is enhanced for daily UV dose data because of the error from representing the entire day's cloud cover based on a single near-noon measurement of the reflectivity. In our station, because of the prevailing clear-sky conditions, noon and daily dose data show very similar comparison statistics. However, the sky conditions during the TOMS overpass and its variability during the interval of Brewer measurements are a notable noise source in the TOMS-Brewer comparisons [Martin *et al.*, 2000; Arola *et al.*, 2002]. In this paper, we compare the instantaneous TOMS UV irradiances around solar noon with the averages of Brewer measurements between 11 and 13 hours. In order to analyze the influence of this Brewer temporal sampling over TOMS-Brewer differences, we have added to Figures 3a and 4a the dependence of the CRV on the TOMS reflectivity. CRV is calculated for analyzing the variability of Brewer measurements during the 2-hour window. It is defined as $CRV = 100 \times SD/M$, where M and SD are the mean and the standard deviation, respectively, of the Brewer measurements between the 11 and 13 hours. During these two hours, the CRV parameter gives information about cloud variability.

[35] Both Figures 3a and 4a show that the CRV values are low when TOMS LER is low. This fact indicates that if the sky was cloud-free at TOMS overpass, the Brewer values do not present a significant variability. Therefore the overestimation of Brewer values by TOMS data obtained for cloud-free conditions are not attributed to the Brewer temporal sampling. In contrast, the cloudiness around TOMS overpass (large values of LER) causes a notable increase of CRV parameter. This rise could be due to the presence of both cloudy and cloud-free conditions during the two hours of Brewer measurements. Therefore clouds around TOMS overpass time tend to increase the Brewer averages and reduce the TOMS-Brewer differences. This effect could explain part of the decrease in TOMS-Brewer bias obtained for large TOMS-LER values as shown Figures 3a and 4a.

[36] In addition, Figures 3b and 4b show frequency distribution (histograms) of the TOMS-Brewer bias at our site. In the distribution of the bias occurrence, one can observe the compensating effect of positive and negative values that gives the overall comparison statistics shown in

Table 3 [evaluated with expression (4)]. However, not all previous studies examined the UV TOMS bias versus cloudiness and associated histograms, which facilitates the comparison between different sites. As can be seen, depending on the total number, relative weight (more summer than winter data), outliers, etc., of data taken at each site, one can obtain quite different TOMS bias (MBE) at different sites and at different seasons for all sky conditions.

[37] For example, Figure 3a can be compared with Figure 4 in the work of Kalliskota *et al.* [2000] showing TOMS comparisons of CIE daily dose at three stations: Ushuaia, Palmer, and San Diego. In San Diego, there are few data, giving a positive bias, similar to our site. Negative bias values were obtained for Ushuaia and Palmer, which are mainly explained by the snow albedo

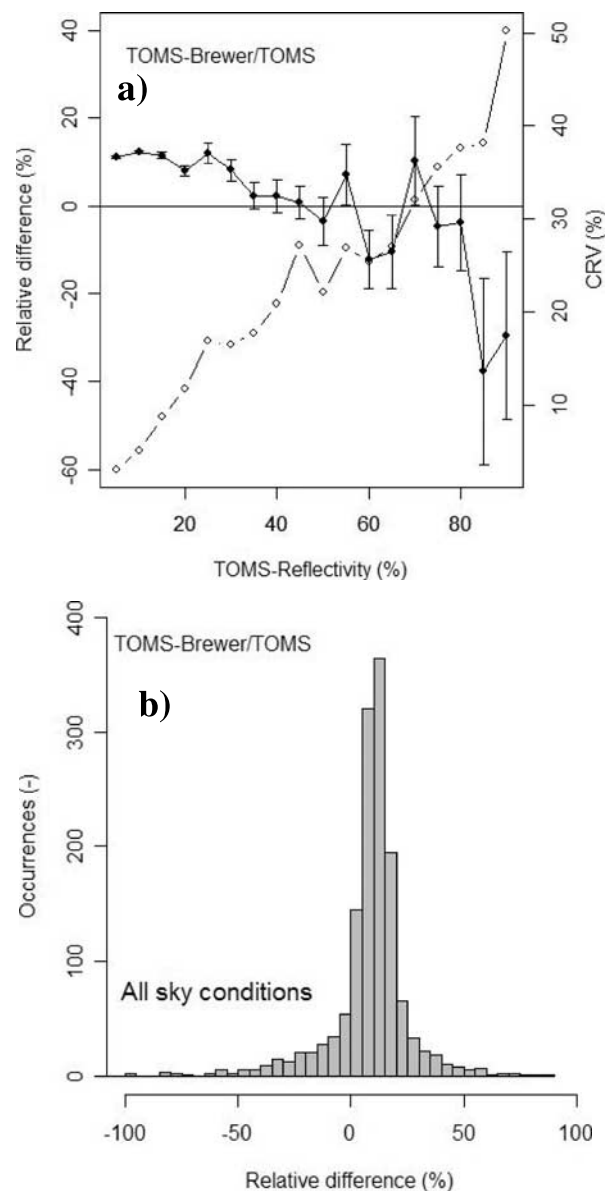


Figure 3. (a) Dependence of the relative difference between TOMS and Brewer noon CIE irradiance (normalized to TOMS data) for all sky conditions with the TOMS reflectivity. (b) Occurrence histogram of TOMS bias.

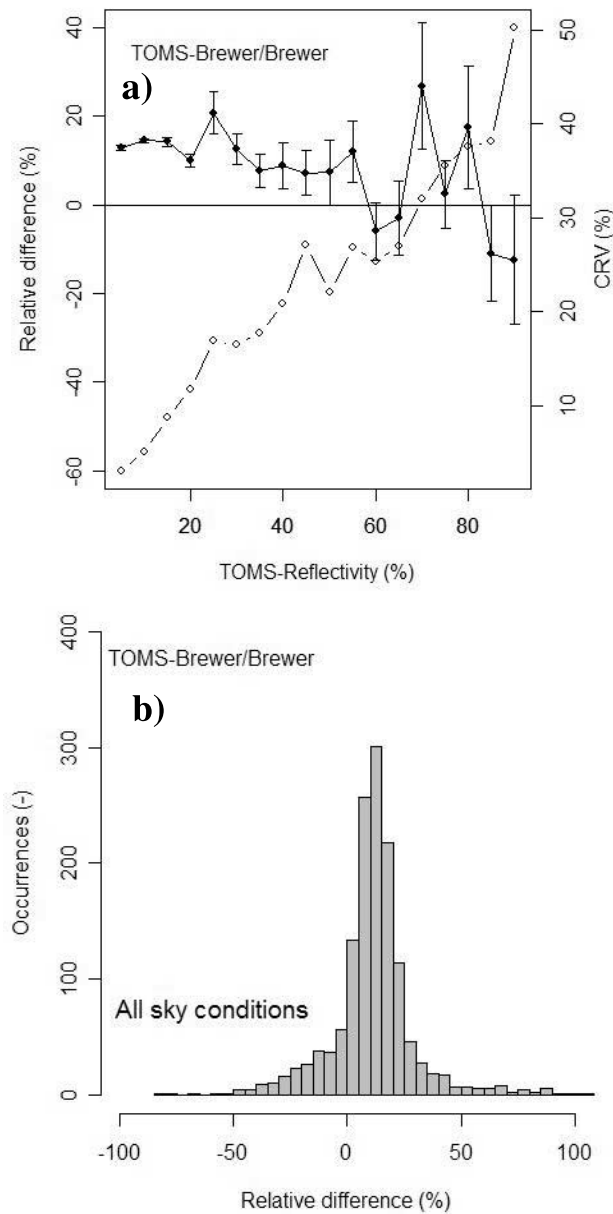


Figure 4. (a) Dependence of the relative difference between TOMS and Brewer noon CIE irradiance (normalized to Brewer data) for all sky conditions with the TOMS reflectivity. (b) Occurrence histogram of TOMS bias.

influence, which is a completely different problem. As was demonstrated in previous studies [Krotkov *et al.*, 2001a, 2001b, 2002; Chubarova *et al.*, 2002; Arola *et al.*, 2003], snow cover can result in both positive and negative bias depending on whether TOMS underestimates or overestimates surface albedo. Therefore the TOMS bias at Ushuaia and Palmer can be explained by a combined effect of snow cover and cloudy conditions. We also found the TOMS bias dependence on reflectivity in the work of Cede *et al.* [2004, Figure 3] for some Argentine stations, some of them with similar climatological characteristics to our station. However, the bias estimated by Cede *et al.* is independent of TOMS reflectivity for most of the stations, contrary to our and other results [Kalliskota *et al.*, 2000; Chubarova *et al.*, 2002]. Chubarova *et al.* [2002] analyzed the dependence of TOMS bias as a function of LER but found only positive bias, which increases considerably for LER > 90%. The latter behavior may be due to high uncertainty because it shows a contrary trend to our results and that of Kalliskota *et al.*, while in the work of Cede *et al.*, one can observe all types of LER dependence.

[38] Most recently, Kazantzidis *et al.* [2006] analyzed summer data averaged for three European stations (Thessaloniki, Greece; Ispra, Italy; and Bilthoven, Netherlands) and showed mainly positive bias with a weak dependence on cloud optical depth (correlated with TOMS reflectivity). Their results reflect the prevailing clear-sky conditions where the few negative values are compensated for in the average of the three stations during summer conditions.

[39] Figure 5 shows that the seasonal dependence of the monthly mean MBE for noon CIE irradiance is anticorrelated with the monthly cloud occurrences (the difference between the total number of data minus the number of data for cloud-free conditions). The lowest MBE values in March (~5%) and October–December are associated with high cloud occurrence, while largest TOMS bias in July–September period (10–15%) is associated with low cloud occurrences. Hence the seasonal dependence is clearly explained by occurrence of clouds but also may be due to the observed seasonal cycle of aerosol absorption as suggested by Krotkov *et al.* [2005a] and Arola *et al.* [2005] and specifically by desert dust aerosol absorption typical for this area as discussed by Toledano *et al.* [2006] (see later aerosol discussion).

[40] Note that we have not mentioned the remaining positive TOMS bias due to absorbing aerosol because we are focused on the analysis of cloud effects as the major influence under all sky conditions. Absorbing aerosols are very important at polluted sites [Krotkov *et al.*, 2002, 2005a; Chubarova *et al.*, 2002] or in areas with a significant load of mineral dust (e.g., Mediterranean areas) under prevailing cloud-free conditions.

Table 3. Daily and Monthly Statistical Parameters of Relative Differences TOMS-Brewer Noon CIE Irradiance and Daily CIE Dose for All Sky Conditions for the Whole Period 2000–2004

	<i>N</i>	Mean, %	SE, %	Median, %	<i>P</i> ₉₀ , %	<i>P</i> ₁₀ , %
Noon Values	1428	7.5	0.7	10.2	21.9	−9.2
Monthly Averages Values	57	9.5	0.6	9.1	14.5	4.1
Daily Dose Values	1393	8.3	0.6	10.8	23.9	−7.6
Monthly Averages Values	57	10.7	0.7	10.5	16.0	5.0

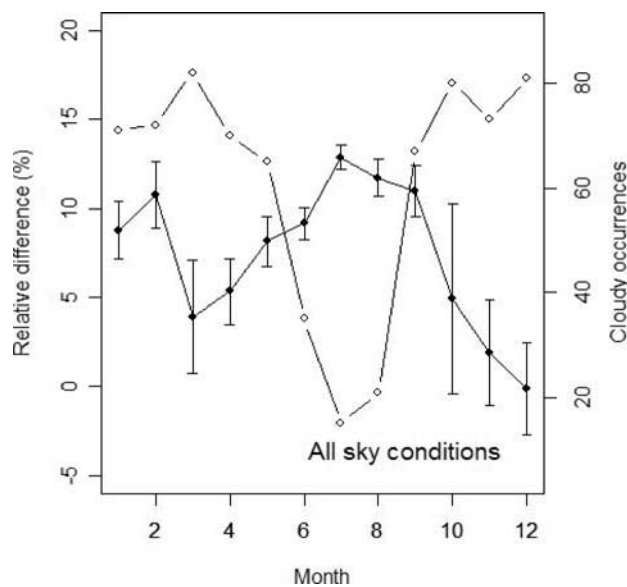


Figure 5. Monthly evolution of the relative difference between TOMS and Brewer noon UV irradiance for all sky conditions. At the right axis, the number of occurrences per month for cloudy conditions, given by the difference between total number of data for all sky conditions minus number of data for cloud-free conditions.

[41] The notable reduction of error bars in summer months is due to less cloud contamination of the scene seen by TOMS. Several statistical parameters are shown in Table 3 for noon CIE irradiance and daily CIE dose. Both statistics are similar. These results represent all available data (one value for each day) and monthly average data, with a total of 1428 (1393 for CIE dose) days and 57 months. For daily data, the MBE parameter is notably lower (7.5% for noon CIE data and 8.3% for CIE doses) than the median of the bias (10.2% for noon CIE data and 10.8 for CIE doses). In contrast, for monthly data, the mean and median values are very similar for noon CIE data as for CIE doses. Moreover, for monthly cases, the MBE parameter is slightly higher than for daily data. Thus daily data are affected more strongly by cloudiness than monthly data.

[42] On the other hand, for monthly average data, the differences between percentiles 90 and 10 are 10.4 and 11.0% for noon CIE irradiance and daily UV dose, respectively. For all data, the differences between percentile 90 and 10 are 31.1% for noon CIE irradiance and 31.5% for daily CIE dose. Therefore the scatter of all data is substantially reduced in the monthly average. The observed seasonal dependences (lower positive bias in spring and fall-winter months) are similar to previous studies [i.e., Fioletov et al., 2002; Chubarova et al., 2005].

[43] The positive clear-sky bias of TOMS-Brewer (or other ground radiometric systems) agrees with our results, but it is very variable depending on the site from about 5 to 30%. However, this bias shows a strong dependence on reflectivity, given positive values for low-medium reflectivity and negative values for high (generally greater than 80%) or strong cloudy conditions. The intermedium reflectance values (40–80%) may give a positive or negative bias

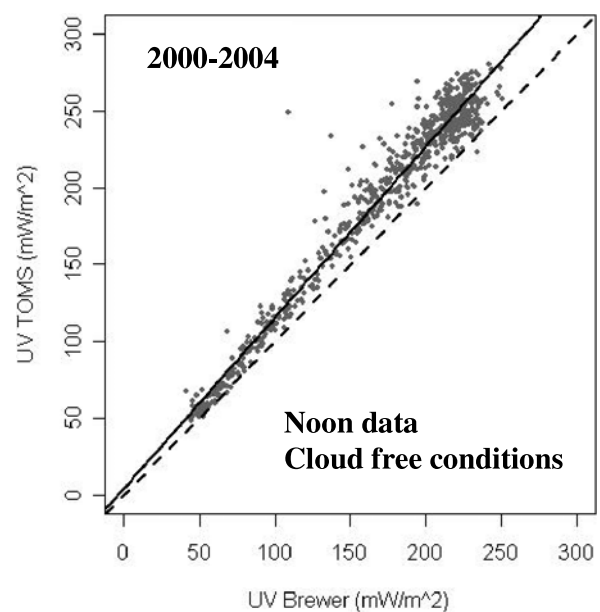


Figure 6. Regression between TOMS and Brewer noon UV irradiance for cloud-free conditions. As above, the solid line is the least square linear regression line, and the dashed line symbolizes the ideal correlation of unit slope.

depending on the prevailing cloud conditions with a strong site dependence. The bias behavior at high reflectivity deserves further study.

4.2. Data Set 2: Cloud-Free Cases

[44] We have taken $LER < 10\%$ over our data set ($\sim 50\%$ of data) as a conservative condition for selecting cloud-free cases according to Kalliskota et al. [2000] instead of 15% by Krotkov et al. [1998]. The TOMS versus Brewer scatterplots is shown in Figure 6 for noon irradiance CIE data. Compared with all sky conditions (Figure 1b), the scatter is considerably decreased, although the bias remains and becomes more significant (often referred to as the clear-sky bias [Fioletov et al., 2004]). This demonstrates that clouds are not the main reason for TOMS-GB bias as mentioned above, and it must be due to aerosol absorption [Krotkov et al., 2005a; Arola et al., 2005]. Table 4 shows the regression statistics for cloud-free conditions containing a free intercept fit and one constrained to pass through the origin. Table 5 shows the statistical parameters of the relative differences between satellite and ground-based data.

[45] The regression errors referring to the free intercept case are lower ($RMSE = 7.7\%$) for cloud-free days than for all sky conditions ($RMSE = 29.5\%$), which is consistent with the assumption that clouds are the main source of the scatter between satellite and GB UV data. However, the

Table 4. Results of the Regression Line TOMS-Brewer Noon CIE Irradiance for Cloud-Free Conditions for the Period 2000–2004^a

	<i>N</i>	Slope	SLE (Slope)	<i>Y</i> Intercept, mW/m^2	INE (<i>Y</i> Intercept), mW/m^2	R^2	RMSE, %
Noon	696	1.11	0.01	4.2	1.6	0.96	7.1
		1.11	0.01	0	0	0.99	6.8

^a Last line gives the regression line constrained to pass through the origin.

Table 5. Daily and Monthly Statistical Parameters of Relative Differences Between TOMS-Brewer Noon Erythemal-CIE Irradiance for Cloud-Free Conditions for the Period 2000–2004

	<i>N</i>	Mean, %	SE, %	Median, %	<i>P</i> ₉₀ , %	<i>P</i> ₁₀ , %
Noon Values	696	11.8	0.2	11.5	18.2	5.1
Monthly Averages Values	57	11.4	0.5	11.6	15.4	6.5

MBE for cloud-free days ($11.8 \pm 0.2\%$) is higher than for all sky conditions ($7.5 \pm 0.7\%$, see Table 3) since the compensating effect of cloudiness is not anymore applicable (Figure 3a).

[46] Also, according to Table 5, when daily cloud-free cases are considered, the difference between percentile 90 and 10 is 13.1% compared to 9.9% when monthly averages are taken. Therefore for the cloud-free data set, the dispersion is reduced but to a lesser extent when considering monthly averages. As above, the seasonal dependence of the monthly MBE for noon CIE is presented in Figure 7, showing a slightly different pattern compared to the all sky conditions of Figure 5. The spring minimum (March in Figure 5) shifts to the winter season (December), and the summer maximum shifts to the early fall (September), but the amplitude of the seasonal cycle has decreased. As before, the seasonal tendency is modulated both by the number of cloud-free data and the cycle of the aerosol absorption as suggested by *Krotkov et al.* [2005a], *Arola et al.* [2005], and specifically by desert dust aerosol absorption typical for this area as discussed by *Toledano et al.* [2006]. The standard errors of the monthly MBE have been reduced remarkably.

4.3. Aerosol Effects

[47] Because of continuous monitoring of aerosol by the AERONET data, we conducted a detailed analysis of the

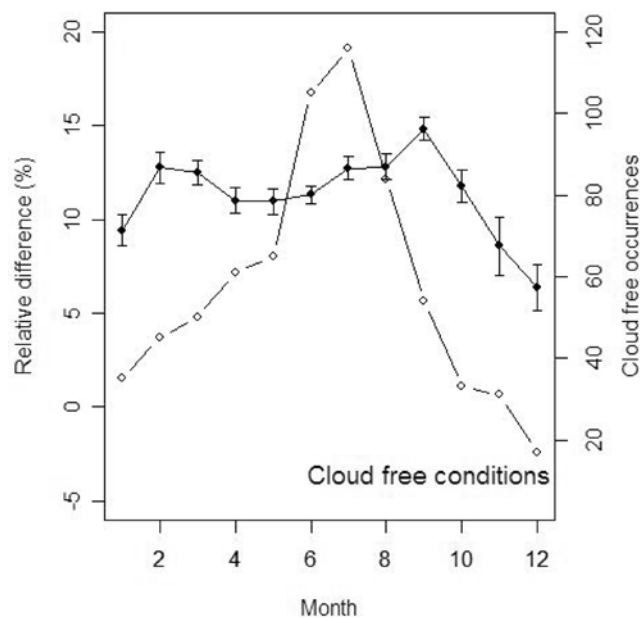


Figure 7. Monthly evolution of the relative difference between TOMS and Brewer noon UV irradiance for cloud-free conditions. At the right axis, the number of occurrences per month for cloud-free conditions.

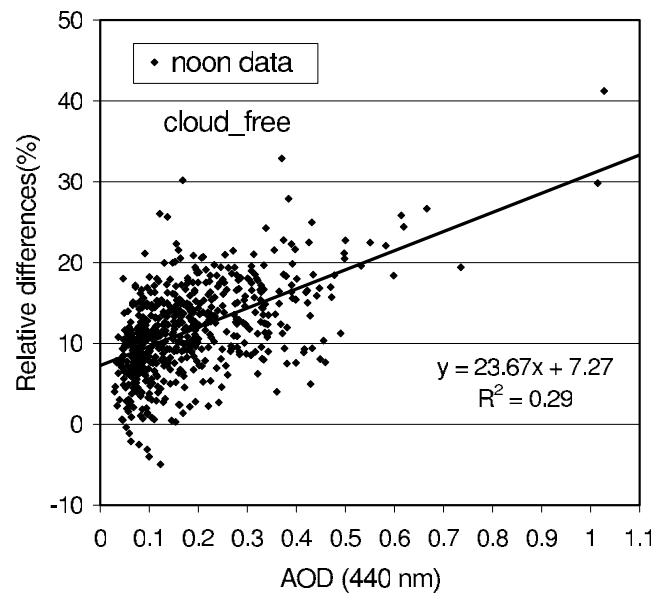


Figure 8. Dependence of the relative difference between Brewer and TOMS noon UV irradiance as a function of aerosol optical depth for all data points.

TOMS-Brewer bias (MBE) as a function of the extinction AOT (or AOD, indifferently). Unfortunately, our Cimel is not equipped with UV filters, so the shortest channel used for analysis was centered at 440 nm (FWHM = 10 nm). Figure 8 shows the bias (MBE) dependence on AOT for noon CIE irradiance taking all available data. Because of the observed low correlation ($R^2 = 0.29$), the MBE was calculated, binning the data with a 0.05 AOT bin as shown in Figure 9. The height of boxes in Figure 9 corresponds to MBE values for each AOT bin. The error bars show the SE

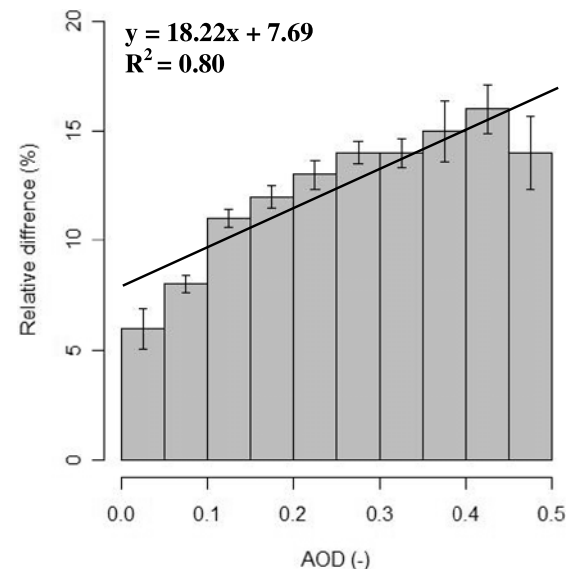


Figure 9. Dependence of the binned relative difference between Brewer and TOMS noon UV irradiance as a function of aerosol optical depth, taking 0.05 bins of AOT data. Bias dependence on the binned AOT for cloud-free subset.

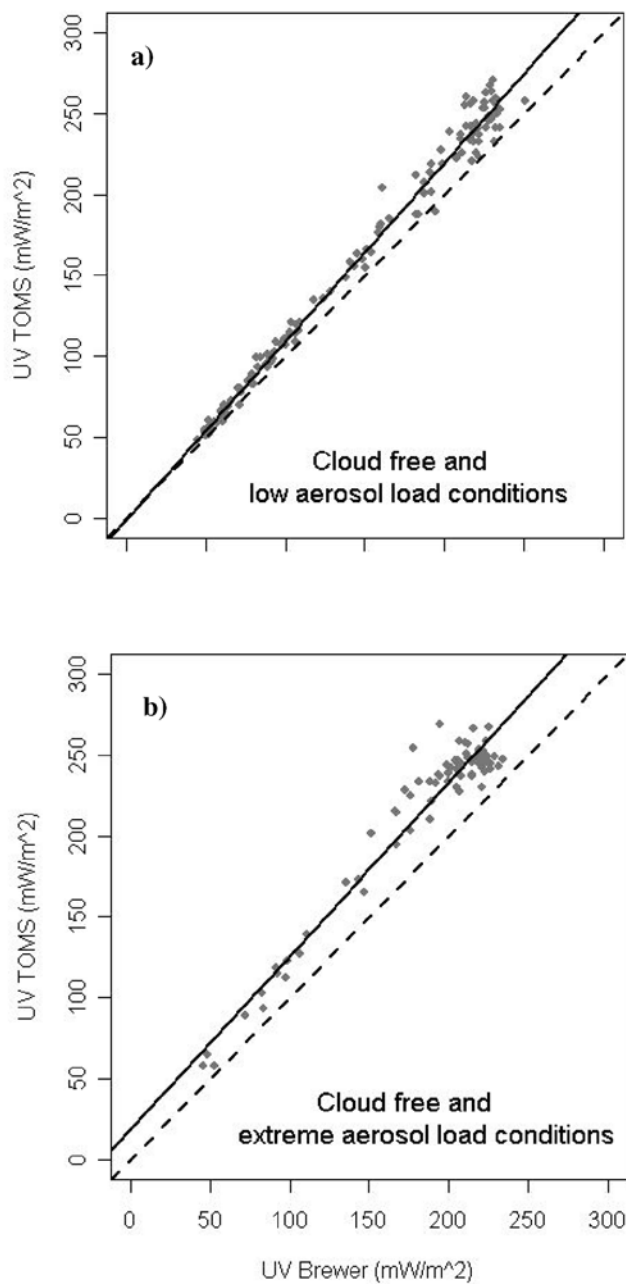


Figure 10. Regression between TOMS and Brewer for noon UV irradiance for cloud-free conditions (a) with low aerosol load and (b) with extreme aerosol load.

of the differences for each AOT bin. The correlation between binned MBE and AOT is improved: $R^2 \sim 0.8$. The bias increases steadily with AOT, from 8% for AOT = 0.1 to 15% for AOT = 0.45. The observed lower box for the 0.5 bin may be due to the applied aerosol correction in the UV TOMS algorithm for AI higher than 0.5. These AI values correspond to a high percentage of AOT values higher than 0.4, although there is no correlation between AI and AOT values for our database (figure not shown).

[48] These results indicate that TOMS estimates are very sensitive to aerosol load in the troposphere. As mentioned in the works of Krotkov *et al.* [1998, 2005a], if absorption by aerosols is underestimated, the TOMS CT value is over-

Table 6. Results of the Regression Line TOMS Versus Brewer Noon CIE Irradiance for Cloud-Free Conditions with Low Aerosol Load for the Period 2000–2004^a

N	Slope	SLE (Slope)	Y Intercept, mW/m ²	INE (Y Intercept), mW/m ²	R^2	RMSE, %
133	1.10	0.01	−1.1	1.7	0.98	4.6
	1.10	0.01	0	0	0.99	4.8

^aThird line gives the regression line constrained to pass through the origin.

estimated; therefore TOMS CIE data are biased high. Similar comparisons [Meloni *et al.*, 2005; Kazantzidis *et al.*, 2006; Arola *et al.*, 2005] also found correlation between TOMS bias and AOT but with correlation coefficients between 0.3 and 0.6.

[49] Krotkov *et al.* [2004, 2005a] suggested that TOMS UV bias is better correlated with aerosol absorption optical thickness (AAOT), which can be explained by true aerosol absorption in the boundary layer not accounted by the TOMS operational UV algorithm. They have developed a new technique to measure column AAOT and single-scattering albedo in the UV by combining UV Multifilter Rotating Shadowband radiometer (UV-MFRSR) data with colocated AERONET aerosol measurements, Brewer direct Sun ozone and NO₂ measurements, and radiative transfer modeling [Krotkov *et al.*, 2005a, 2005b], and suggested simple off-line correction to the TOMS data. In similar TOMS-Brewer comparisons, Arola *et al.* [2005] also correlated TOMS surface UV bias with the AAOT measured by the same Brewer instrument. Their study was conducted at two stations: Ispra in Italy and Thessaloniki in Greece, and they arrived at the similar conclusion that the AAOT is better correlated with the TOMS bias than aerosol extinction optical thickness or aerosol single-scattering albedo. At our station, a similar work is planned in the future when reliable AAOT data will become available. Here we present only an analysis with aerosol extinction AOT data.

4.3.1. Data Set 3: Cloud-Free Cases With Low Aerosol Load

[50] Figure 10a shows the scatterplot between TOMS and Brewer for noon CIE irradiance data when only low aerosol loads (AOT < 0.1) are considered. These atmospheric conditions are closer to the TOMS model, when the best agreement with GB measurements is expected. Indeed, the correlation is excellent ($R^2 = 0.98$) as is illustrated in Table 6 (the same parameters are shown for the fit constrained to pass by the origin but not discussed). If Figure 10a and Tables 6 and 7 are compared with the above equivalent figures and tables, it is observable that the noise has

Table 7. Daily and Monthly Statistical Parameters of Relative Differences Between Brewer and TOMS Noon Erythemal-CIE Irradiance for Cloud-Free Conditions with Low Aerosol Load for the Period 2000–2004

	N	Mean, %	SE, %	Median, %	P_{90} , %	P_{10} , %
Daily Values	133	8.2	0.4	8.2	13.7	2.3
Monthly Averages Values	46	8.6	0.5	8.6	11.8	4.8

Table 8. Results of the Regression Line TOMS Versus Brewer Noon CIE Irradiance for Cloud-Free Conditions with Extreme Aerosol Load for the Whole Period 2000–2004^a

N	Slope	SLE (Slope)	Y Intercept, mW/m ²	INE (Y Intercept), mW/m ²	R ²	RMSE, %
73	1.07	0.03	18.4	6.1	0.94	7.4
	1.17	0.01	0	0	0.99	11.9

^a Last line gives the regression line constrained to pass through the origin.

decreased considerably. This result is expected: as aerosol and cloud effects are removed, the differences between satellite and ground-based measurements are reduced to the measured uncertainties [Cede *et al.*, 2004, Table 5; Krotkov *et al.*, 1998, Table 3].

[51] The MBE for cloud-free cases with low aerosol load still remains, for example, for noon CIE irradiance, at $8.2 \pm 0.4\%$. The noise RMSE value of 4.6% is lower compared with all aerosol cloud-free conditions (RMSE = 7.1%) and significantly lower compared with all sky conditions (RMSE = 29.5%). To summarize, the cloudiness and aerosols explain about 84% RMSE variation $[(29.5 - 4.6)/29.5 = 84.4\%]$ for TOMS-Brewer noon CIE irradiance data.

[52] It should be noted that Table 3 in the work of Krotkov *et al.* [1998] shows TOMS uncertainties estimated by taking atmospheric transmittance only, not including uncertainty in extraterrestrial solar flux (ETF) data. Including ETF error of 3%, TOMS-estimated absolute CIE uncertainty is $\sim 4\%$ for cloud- and aerosol-free conditions [Krotkov *et al.*, 2001b], which is comparable with observed 4.6% bias in Brewer-TOMS comparisons (note that not all of this bias is due to TOMS, and some part of the bias is also due to the Brewer measurement uncertainties: cosine response, absolute calibration, etc.).

4.3.2. Data Set 4: Cloud-Free Cases With Extreme Aerosol Load

[53] We have analyzed the cases with high aerosol optical depth according the characteristics of aerosol load in our area [Toledano, 2005; Cachorro *et al.*, 2005]. We must emphasize that these extreme AOT cases, with $AOT_{440} > 0.25$ and $\alpha < 0.8$, correspond in 95% of cases to African desert dust outbreaks over our station [Toledano *et al.*, 2006].

[54] Figure 10b shows the TOMS versus Brewer data for this subset, which shows a significant TOMS overestimation, but the correlation remains significant with a R^2 of 0.94 and RMSE values of 7.4%. Other parameters of the regression are shown in Table 8, and Table 9 shows the

Table 9. Daily and Monthly Statistical Parameters of Relative Differences Between Brewer and TOMS Noon Erythral-CIE Irradiance for Cloud-Free Conditions with Extreme Aerosol-Load for the Whole Period 2000–2004

	N	Mean, %	SE, %	Median, %	P ₉₀ , %	P ₁₀ , %
Daily Values	73	15.1	0.7	14.9	22.3	8.1
Monthly Averages Values	32	15.9	0.9	15.9	21.1	9.3

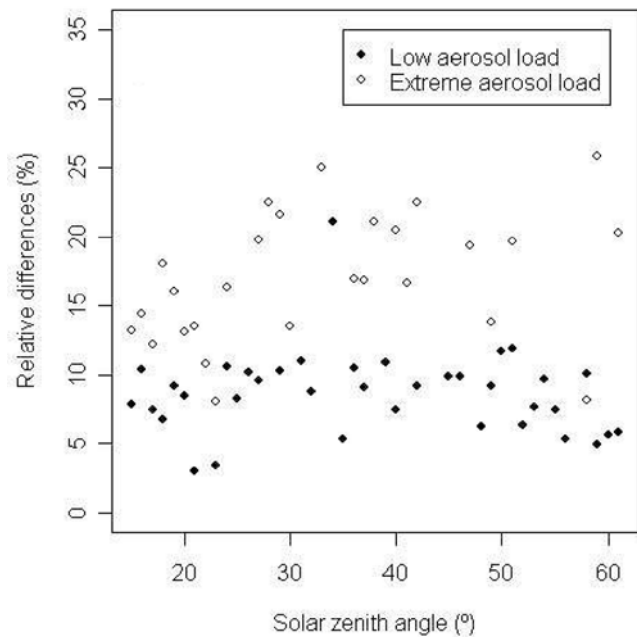


Figure 11. Dependence of the relative differences between Brewer and TOMS noon UV irradiance for cloud-free cases on solar zenith angles during low and extreme aerosol load.

statistical parameters of the comparison. The MBE is higher when aerosol-extreme conditions are considered. For example, the MBE is $8.2 \pm 0.4\%$ for cloud-free with low aerosol load cases to $15.1 \pm 0.6\%$ for extreme aerosol load. It is also clear that most of our data show higher scatter with increasing AOT.

[55] This overestimation is due to the fact that TOMS cannot correctly detect the presence of absorbing aerosols in the boundary layer (urban and industrial aerosol). McKenzie *et al.* [2001] explained better agreement at the clean Lauder (New Zealand) site, compared to Toronto or other polluted European city stations, by pollution effects. Similar to that, Fioletov *et al.* [2004] explained that part of the 10–30% of positive summer bias of TOMS UV compared to Canadian and US Brewer network is also due to absorbing aerosols and pollution effect in the lower troposphere.

[56] In our area, the absorbing aerosols are mostly represented by desert dust aerosols. A detailed inventory of desert dust aerosols by Toledano [2005] shows that these aerosols account for 28% of average AOT climatological levels at 440 nm (48% at 870 nm). These absorbing aerosols attenuate UV radiation more strongly than other aerosol types with the same AOT. This causes an overestimation of C_T factor [equation (1)] and TOMS CIE overestimation. However, the bias can be substantially reduced with off-line absorbing aerosol correction suggested by Arola *et al.* [2005] and Krotkov *et al.* [2005a]. It should be noted, however, that direct measurements of aerosol absorption present a great challenge even for ground-based remote-sensing techniques. The uncertainties have been discussed recently [Bais *et al.*, 2005; Krotkov *et al.*, 2005a; Arola *et al.*, 2005].

[57] Finally, Figure 11 shows the MBE dependence on solar zenith angles during low and extreme aerosol load for the whole period of observations, 2000–2004. The figure shows no statistically significant dependence on

SZA as expected for properly cosine-corrected Brewer data, although the data for extreme aerosol load show increased values and variability.

5. Conclusions

[58] Some important conclusions may be derived from the earlier results of TOMS-Brewer comparison for noon CIE irradiance and daily CIE dose over our area of study in the southwest of Spain, where the number of cloud-free days is high and dust outbreaks are frequent. Earlier comparative works have generally found a positive TOMS versus ground-based measurement bias for noon irradiances and daily dose for all sky conditions. Using TOMS reflectivity as a proxy for cloudiness, we show that the TOMS CIE bias reduces with increased cloudiness compared to cloud-free conditions and even becomes negative for high reflectivity (>80%). Therefore the TOMS bias is reduced when data for all cloud conditions (including high reflectivity) are mixed with cloud-free data. This could also explain, in part, quite different overall TOMS bias values previously obtained at different sites as well as different seasonal dependence of the bias. We also found that the noise in comparisons also increases with increasing LER, in agreement with previous results [i.e., Cede *et al.*, 2004; Kalliskota *et al.*, 2000].

[59] Another relevant point of this analysis is the nearly similar behavior for near-noon and daily data for all sky conditions, which suggests that a single daily TOMS measurement can be considered as an unbiased daily exposure estimator at our site. This is a consequence of the prevailing clear-sky conditions. The noise in TOMS versus GB CIE measurements decreases considerably when cloud-free days are selected for comparison. There is a consistent and significant reduction in RMSE values, implying that (1) local GB UV data better represent larger surrounded area (~100–200 km), and (2) TOMS spatially averaged UV estimates better represent local conditions.

[60] The accuracy of TOMS CIE estimate for cloud-free conditions is best when we select only conditions with low aerosol optical depth; the bias is close to the estimated uncertainties of TOMS UV data (i.e., 4–5%) [Krotkov *et al.*, 2001b]. However, for high aerosol optical depth, the bias increases considerably. This is due to the fact that absorbing aerosols in the boundary layer are currently not adequately modeled in the operational TOMS UV algorithm.

[61] Krotkov *et al.* [2004, 2005a] and Arola *et al.* [2005] have recently suggested off-line correction due to absorbing aerosols if the AAOT is known at the site. The problem is that currently, there are no standard methods of measuring AAOT (or aerosol single-scattering albedo) in the UV wavelengths even from the ground. TOMS AI method provides estimates of AAOT and a simple method of UV irradiance correction when aerosols are elevated to the free troposphere [Krotkov *et al.*, 1998], but the AI method does not work for pollution aerosols that are typically in the boundary layer (below 2 km). New aerosol absorption product from the Aura/OMI instrument (launched in July 2004), if proved sensitive to boundary-layer aerosol, could be used for operational improvement of UV product from Ozone Monitoring Instrument on board of NASA EOS

Aura satellite [Krotkov *et al.*, 2001b]. This is currently a subject of ongoing research.

[62] **Acknowledgments.** This work has been partially granted by the Spanish “Ministerio de Educación y Ciencia” by means of projects AP2001-0845, REN2002-00966/CLI, and coordinated project CGL2005-05693-C03/CLI.

References

- Arola, A., et al. (2002), Assessment of four methods to estimate surface UV radiation using satellite data, by comparison with ground measurements from four stations in Europe, *J. Geophys. Res.*, **107**(D16), 4333, doi:10.1029/2001JD000462.
- Arola, A., S. Kazadzis, N. Krotkov, A. Bais, J. Gröbner, and J. R. Herman (2005), Assessment of TOMS UV bias due to absorbing aerosols, *J. Geophys. Res.*, **110**, D23211, doi:10.1029/2005JD005913.
- Arola, A., J. Kaurola, L. Koskinen, A. Tanskanen, T. Tikkanen, P. Taalas, J. R. Herman, N. Krotkov, and V. Fioletov (2003), A new approach to estimating the albedo for snow-covered surfaces in the satellite UV method, *J. Geophys. Res.*, **108**(D17), 4531, doi:10.1029/2003JD003492.
- American Cancer Society (ACS) (2004), Cancer facts and figures, *Technical report 2004*, American Cancer Society, Atlanta, Georgia, USA.
- Bais, A. F., A. Kazantzidis, S. Kazadzis, D. S. Balis, C. S. Zerefos, and C. Meleti (2005), Deriving an effective aerosol single scattering albedo from spectral surface UV irradiance measurements, *Atmos. Environ.*, **39**(6), 1093–1102.
- Cachorro, V. E., C. Toledano, R. Vergaz, A. M. de Frutos, M. Sorribas, J. M. Vilaplana, and B. A. de la Morena (2005), The Photons-Aeronet network stations in Spain, in *Recent Advances in Multidisciplinary Applied Physics*, edited by A. Méndez-Vilas, Elsevier, New York.
- Cachorro, V. E., R. Vergaz, A. M. de Frutos, J. M. Vilaplana, D. Henriques, N. Laulainen, and C. Toledano (2006), Study of desert dust events in the southwestern of the Iberian Peninsula in year 2000: Two case studies, *Ann. Geophys.*, **24**, 1–18.
- Cede, A., E. Luccini, L. Nuñez, R. D. Pianceti, M. Blumthaler, and J. R. Herman (2004), TOMS-derived erythema irradiance versus measurements at stations of Argentine UV Monitoring Network, *J. Geophys. Res.*, **109**, D08109, doi:10.1029/2004JD004519.
- Chubarova, N. Y., A. Y. Yurova, N. Krotkov, J. R. Herman, and P. K. Barthia (2002), Comparison between ground measurements of broadband ultraviolet irradiance (300 to 380 nm) and total ozone mapping spectrometer ultraviolet estimates at Moscow from 1979 to 2000, *Opt. Eng.*, **41**, 3070–3081.
- Chubarova, N. Y., Y. E. Nezval, J. Verdebout, N. Krotkov, and J. Herman (2005), Long-term UV irradiance changes over Moscow and comparison with UV estimates from TOMS and METEOSAT, in *Proc. Ultraviolet Ground- and Space-based Measurements, Models, and Effects V*, edited by G. Bernhard, J. R. Slusser, J. R. Herman, and W. Gao, pp. 63–73, SPIE, San Diego, USA.
- Dave, J. V. (1964), Meaning of the successive iteration of the auxiliary equation of the radiative transfer, *Astrophys. J.*, **140**, 1292–1303.
- Diffey, B. L. (1991), Solar ultraviolet radiation effects on biological systems, *Phys. Med. Biol.*, **36**, 299–328.
- Fioletov, V. E., J. B. Kerr, D. I. Wardle, N. Krotkov, and J. R. Herman (2002), Comparison of Brewer ultraviolet irradiance measurements with total ozone mapping spectrometer satellite retrievals, *Opt. Eng.*, **41**, 3051–3061.
- Fioletov, V. E., M. G. Kimlin, N. Krotkov, L. J. B. McArthur, J. B. Kerr, D. I. Wardle, J. R. Herman, R. Meltzer, T. W. Mathews, and J. Kaurola (2004), UV index climatology over the United States and Canada from ground-based and satellite estimates, *J. Geophys. Res.*, **109**, D22308, doi:10.1029/2004JD004820.
- Herman, J. R., and E. Celarier (1997), Earth surface reflectivity climatology at 340 to 380 nm from TOMS data, *J. Geophys. Res.*, **102**, 28,003–28,011.
- Herman, J. R., N. A. Krotkov, E. Celarier, D. Larko, and G. Labow (1999), The distribution of UV radiation at the Earth's surface from TOMS measured UV-backscattered radiances, *J. Geophys. Res.*, **104**, 12,059–12,076.
- Holben, B. N., et al. (1998), AERONET—A federated instrument network and data archive for aerosol characterization, *Remote Sens. Environ.*, **66**, 1–16.
- Kalliskota, S., J. Kaurola, P. Taalas, J. Herman, E. Celarier, and N. Krotkov (2000), Comparison of daily UV doses estimated from Nimbus 7/TOMS measurements and ground-based spectroradiometer data, *J. Geophys. Res.*, **105**, 4273–4277.
- Kazantzidis, A., et al. (2006), Comparison of satellite-derived UV irradiances with ground-based measurements at four European stations, *J. Geophys. Res.*, **111**, D13207, doi:10.1029/2005JD006672.

- Krotkov, N. A., P. K. Barthia, J. R. Herman, V. Fioletov, and J. Kerr (1998), Satellite estimation of spectral surface UV irradiance in the presence of tropospheric aerosols, *J. Geophys. Res.*, **103**, 8779–8793.
- Krotkov, N. A., J. R. Herman, P. K. Barthia, V. Fioletov, and Z. Ahmad (2001a), Satellite estimation of spectral surface UV irradiance 2. Effects of homogeneous clouds and snow, *J. Geophys. Res.*, **106**, 11,743–11,759.
- Krotkov, et al. (2001b), ATBD-OMI-03, on line document (2001) [http://eosps0.gsfc.nasa.gov/eos_homepage/for_scientists/atbd/viewInstrument.php?instrument=13].
- Krotkov, N. A., J. R. Herman, P. K. Barthia, C. Seftor, A. Arola, J. Kaurola, S. Kalliskota, P. Taalas, and I. V. Geogdzhayev (2002), Version 2 total ozone mapping spectrometer ultraviolet algorithm: Problems and enhancements, *Opt. Eng.*, **41**(12), 3028–3039.
- Krotkov, N., J. Herman, V. Fioletov, C. Seftor, D. Larko, A. Vasilkov, and G. Labow (2004), Boundary layer absorbing aerosol correction of an expanded UV irradiance database from satellite Total Ozone Mapping Spectrometer, in *Proceedings of the XX Quadrennial Ozone Symposium*, pp. 1159–1160, June 2004, Kos, Greece.
- Krotkov, N. A., P. K. Barthia, J. R. Herman, J. Slusser, G. Scott, G. Labow, A. P. Vasilkov, T. F. Eck, O. Dubovik, and B. N. Holben (2005a), Aerosol ultraviolet absorption experiment (2000 to 2004), part 2: Absorption optical thickness, refractive index, and single scattering albedo, *Opt. Eng.*, **44**(4), 041005.
- Krotkov, N., J. Herman, A. Cede, and G. Labow (2005b), Partitioning between aerosol and NO₂ absorption in the UVA, in *Ultraviolet Ground- and Space-based Measurements, Models, and Effects V*, edited by Germar Bernhard, James R. Slusser, Jay R. Herman, Wei Gao, pp. 5886, SPIE, San Diego, USA.
- Leszczynski, K., K. Jokela, L. Ylianttila, R. Visuri, and M. Blumthaler (1998), Erythemally weighted radiometers in solar UV monitoring: Results from the WMO/STUK intercomparison, *Photochem. Photobiol.*, **67**(2), 212–221.
- Martin, T. J., B. G. Gardiner, and G. Seckmeyer (2000), Uncertainties in satellite-derived estimates of surfaces UV doses, *J. Geophys. Res.*, **105**, 27,005–27,011.
- Mayer, B., and A. Kylling (2005), The libRadtran software package for radiative transfer calculations—Description and examples of use, *Atmos. Chem. Phys.*, **5**, 1319–1381.
- McKenzie, R. L., G. Seckmeyer, A. F. Bais, J. B. Kerr, and S. Madronich (2001), Satellite retrievals of erythral UV dose compared with ground-based measurements at northern and southern midlatitudes, *J. Geophys. Res.*, **106**, 24,051–24,062.
- McKinlay, A. F., and B. L. Diffey (1987), A reference spectrum for ultraviolet induced erythema in human skin, *CIE-J.*, **6**, 21–27.
- McPeters, R. D., P. K. Barthia, A. J. Krueger, J. R. Herman, C. G. Wellemeyer, G. Seftor, C. F. Jaross, O. Torres, L. Moy, G. Labow, W. Byerly, S. L. Taylor, T. Swisler, and R. P. Cebula (1998), Earth Probe Total Ozone Mapping Spectrometer (TOMS) data products user guide, *Technical report TP-1998-206895*, NASA.
- Meloni, D., A. di Sarra, J. R. Herman, F. Monteleone, and S. Piaentino (2005), Comparison of ground-based and total ozone mapping spectrometer erythral UV doses at the Island of Lampedusa in the period 1998–2003: Role of tropospheric aerosols, *J. Geophys. Res.*, **110**, D01202, doi:10.1029/2004JD005283.
- Sabburg, J., J. E. Rives, R. S. Meltzer, T. Taylor, G. Schmalzle, S. Zheng, N. Huang, A. Wilson, and P. M. Udelhofen (2002), Comparison of corrected daily integrated erythral data from the U. S. E.PA/UGA network of Brewer spectroradiometer with model and TOMS-inferred data, *J. Geophys. Res.*, **107**(D23), 4676, doi:10.1029/2001JD001565.
- Smirnov, A., B. N. Holben, T. F. Eck, O. Dubovik, and I. Slutsker (2000), Cloud screening and quality control algorithms for the AERONET database, *Remote Sens. Environ.*, **73**, 337–349.
- Toledano, C. (2005), Climatología de los aerosoles mediante la caracterización de propiedades ópticas y masas de aire en la estación “El Arenosillo” de la red AERONET, Ph.D. Dissertation, Universidad de Valladolid, Spain.
- Toledano, C., V. E. Cachorro, A. M. de Frutos, and M. Sorribas y B. A. de la Morena (2006), Inventario de episodios de aerosol desértico en el suroeste de la Península Ibérica en el período 2000–2004 a partir de medidas fotométricas de la red AERONET, in *5^o Asamblea Hispano-Portuguesa de Geodesia y Geofísica*, Sevilla, Spain, in press.
- Vilaplana, J. M. (2004), Medida y análisis de ozono y de la radiación solar ultravioleta en El Arenosillo-INTA, Ph.D. dissertation, Universidad de Valladolid, Huelva.
- Vilaplana, J. M., V. E. Cachorro, M. Sorribas, E. Luccini, A. M. de Frutos, A. Berjón, and B. de la Morena (2006), Contribution to calibration procedures for a YES-UVB-1 biometer based on spectral measurements with a Brewer spectrophotometer, *Photochem. Photobiol.*, **82**, 508–514, doi:10.1562/2005-06-23-RA-590.
- Williams, J. E., P. N. den Outer, H. Slaper, J. Matthijsen, and G. Kelfkens (2004), Cloud induced reduction of solar UV-radiation: A comparison of ground-based and satellite based approaches, *Geophys. Res. Lett.*, **31**, L03104, doi:10.1029/2003GL018242.
- WMO (1996), WMO-UMAP Workshop on Broad-band UV Radiometers, Global Atmosphere Watch, *Technical Report #120*, World Meteorological Organization (WMO).
- WMO (2003), Scientific Assessment of Ozone Depletion: 2002 Global Ozone Research and Monitoring Project, *Technical Report #47*, World Meteorological Organization (WMO).
- M. Antón and A. Serrano, Departamento de Física, Universidad de Extremadura, Badajoz, Spain.
- V. Cachorro and C. Toledano, Departamento de Física Teórica, Atómica y Óptica, Universidad de Valladolid, 47071, Valladolid, Spain. (chiqui@baraja.opt.cie.uva.es)
- B. de la Morena and J. M. Vilaplana, ESAt “El Arenosillo”, Instituto Nacional de Técnica Aeroespacial, Huelva, Spain.
- J. R. Herman, Laboratory of Atmosphere, NASA/Goddard Space Flight Center, Greenbelt, MD, USA.
- N. A. Krotkov, Goddard Earth Sciences and Technology Center, University of Maryland, Baltimore, MD, USA.